Approach to the Direct Intramolecular Localization of Antigenic Determinants in *Androctonus australis* Hemocyanin with Monoclonal Antibodies by Molecular Immunoelectron Microscopy†

Jean Lamy,* Josette Lamy, Philippe Billiald, Pierre-Yves Sizaret,‡ Guy Cavé,§ Joachim Frank,‖ and Geneviève Motta⊥

Laboratoire de Biochimie, Faculté de Pharmacie, 37032 Tours Cedex, France

Received December 12, 1984

ABSTRACT: Monoclonal antibodies (mAb) directed vs. subunits from hemocyanin (Hc) of the scorpion *Androctonus australis* were used in molecular immunoelectron microscopy (MIEM) to directly localize the epitopes within the subunits. Four types of mAb were used. First, mAb 6302, an IgG clone highly specific for subunit Aa 2, produced with native hemocyanin long strings composed of hemocyanin molecules in the side view and in the 45° view. At lower concentration, "parachute" and "butterfly" structures composed of two Hc molecules and one monoclonal immunoglobin G (IgG) molecule were obtained. Fab fragments prepared from mAb 6302 bound exactly on the top and bottom edges of the molecule. The second type of mAb (6003), directed vs. subunit Aa 2, produced nice immunocomplexes with the free subunit but nothing with the native oligomer. It is suggested that due to steric hindrance or to conformational changes the epitope is not accessible in the native molecule. The third mAb belonged to the IgM class and apparently bound Hc in the Aa 2 area. However, because of the difficulty of separating the immunocomplexes from the residual mAb and the polymorphism of the IgM molecules, monoclonal IgM are no longer used for MIEM. The last type of mAb (5701) had a high affinity and a high specificity for subunit Aa 6. It produced two types of immunocomplexes with native Hc. The two types differed by a 180° rotation around one of the Fab arms. These complexes, which support recent results of Wrigley et al. [Wrigley, N. G., Brown, E. B., & Skehel, J. J. (1983) *J. Mol. Biol. 169*, 771–774] and of Roux [Roux, K. H. (1983) *Eur. J. Immunol. 14*, 459–464], indicate that monoclonal IgG have a high degree of rotational flexibility around the Fab arm. Monoclonal antibody 5701 bound exactly at the corner of the molecule in the area where subunit Aa 6 is known to be located. The MIEM approach of the location of the epitope requires the model of the architecture and of the quaternary structure to be very precise. Thus, recent findings of Gaykema et al. [Gaykema, W. P. J., Hol, J. M., Vereijken, J. M., Soeter, N. M., Bak, H. J., & Beintema, J. J. (1984) *Nature (London) 309*, 23–29] and of Van Heel et al. [Van Heel, M., Keegstra, W., Schutter, W., & Van Bruggen, E. F. J. (1983) *Life Chem. Rep., Suppl. Ser. 1*, 69–73] led to a reexamination of previous models. Specifically, the left enantiomorph of the dodecamer was substituted with the right enantiomorph and a distinction between the N- and C-terminal domains was introduced. A comparison of this model to the MIEM picture suggests that the epitopes of mAb 6302 and 5701 are both located in the C-terminal domains of subunits Aa 2 and Aa 6, respectively. The consequences of the reexamination of the architecture model of the quaternary structure of (4 × 6)-mer and (8 × 6)-mer Hc are discussed.

Hemocyanins are blue copper-containing oxygen carriers occurring in arthropods and molluscs. Arthropodan hemocyanins, the matter of this paper, are oligomers containing multiples of six subunits and called (1 × 6)-mer or hexamer, (2 × 6)-mer or dodecamer, (4 × 6)-mer and (8 × 6)-mer, respectively. In addition to these well-known forms, recent results of Mangum et al. (1984) indicate that a (6 × 6)-meric structure occurs in centipedes. The aggregation level and the subunit heterogeneity of hemocyanins depend on their phylogenic origin. For example, the hexameric hemocyanin of the spiny lobster *Panulirus interruptus* is composed of five different monomeric subunits. The dodecameric hemocyanin of the freshwater crayfish *Cherax destructor* contains at least five different monomers. The (4 × 6)-mers of the scorpion *Androctonus australis* and of the spider *Eurypelma californicum* hemocyanins as well as the (8 × 6)-mers of the horseshoe crabs *Limulus polyphemus* and *Tachypleus tridentatus* are composed of eight, seven, eight, and seven different monomers, respectively, with molecular masses of 65–75 kDa. For more details about subunit heterogeneity, see reviews of Van Holde & Miller (1982) and Ellerton et al. (1983).

A characteristic of the hemocyanin molecule is to be an excellent antigen. This property was used to investigate the subunit heterogeneity of several arthropod hemocyanins (Lamy et al., 1979a–c; Folkerts & Van Eerd, 1981; Jeffrey et al., 1981), to study their phylogenic and structural relatedness (Lamy et al., 1983; Markl et al., 1984), and to prepare the messenger RNA of several subunits (Siggens & Wood, 1982; Vanderbeke et al., 1982, 1983; Alliel et al., 1983; Avissar et al., 1983; Wood, 1983). However, the best application of the immunological properties of Arthropod hemocyanins is

† This work was supported by Grant JE 032613 from CNRS, by Grant AIP-518014 from NSF-CNRS (Cooperative Science Program), and in part by Grant 1 RO1 GM29169 from the National Institutes of Health.

‡ Present address: Laboratoire de Microscopie Electronique, Faculté de Médecine, 37032 Tours Cédex, France.

§ Present address: Laboratoire de Pharmacie Galénique, Faculté de Pharmacie, 37032 Tours Cédex, France.

‖ Present address: Wadsworth Center for Laboratories and Research, State of New York Department of Health, Albany, NY 12201.

⊥ Present address: Laboratoire d'Immunogénétique, Université d'Orléans, 45046 Orléans Cédex, France, and CNRS, C.S.E.A.L., 45045 Orléans Cédex, France.

0006-2960/85/0424-5532$01.50/0

probably the determination by molecular immunoelectron microscopy (MIEM)[1] of the quaternary structure of three hemocyanins that are among the most complex molecules, namely, those from *A. australis*, *E. californicum*, and *L. polyphemus* (Lamy et al., 1981b, 1983; Sizaret et al., 1982; Markl et al., 1981). The principle of the method was to bind Fab fragments made specific for a single subunit onto the native molecule and to observe the label on the contour of the whole molecule in the electron microscope. Even though spectacular results have been obtained, the resolution of the method was limited to the localization of a subunit within the whole molecule for two reasons. First, the three-dimensional structure of the subunits was unknown, and second, the antibodies used to label the subunits were polyclonal antibodies freed by immunoadsorption of antibodies cross-reacting with other subunits.

Recently, two improvements allowed us to bypass these limitations. First, Gaykema et al. (1984) determined by X-ray crystallography the first three-dimensional structure of a hemocyanin subunit, and the homology between the first amino acid sequences of hemocyanin subunits suggests that probably the hemocyanin folding of *P. interruptus* hemocyanin is general in arthropod hemocyanin (Moore & Riggs, 1982; Nemoto & Takagi, 1982; Schartau et al., 1983; Schneider et al., 1983; Gaykema et al., 1984; Yokota & Riggs, 1984). Second, monoclonal antibodies (mAb) directed vs. hemocyanin subunits have been prepared. In contrast to purified polyclonal antibodies, which allow at most one subunit within an oligomer to be localized, mAb allow a single epitope within a single subunit as well as an epitope within an oligomer to be labeled. This paper presents some characteristic cases of antigenic determinant immunolabeling within native *A. australis* hemocyanin and shows how in the near future it is conceivable that an epitope may be directly localized within a complex antigen.

Materials and Methods

Hemocyanin. Whole hemocyanins of *A. australis* and *L. polyphemus* were prepared as previously reported (Lamy et al., 1979a,b). The (4 × 6)-meric hemocyanin of *A. australis* was dissociated into monomeric and dimeric subunits through an overnight dialysis against a 0.05 M Tris-HCl buffer, pH 8.9, containing 10 mM EDTA, and the residual oligomeric material was removed by gel filtration on Sephadex G-200 in the same buffer. Eight monomeric subunits compose *A. australis* hemocyanin; they are numbered 2, 3A, 3B, 3C, 4, 5A, 5B, and 6 and are prefixed Aa for *Androctonus australis*. When necessary, they were purified according to a previously published method (Lamy et al., 1979a). ^{125}I-labeled isolated subunits were prepared according to the method of Greenwood et al. (1963). Dodecameric quarters of molecule from *L. polyphemus* hemocyanin were obtained by a dialysis against a $I = 0.1$ acetate buffer, pH 5.0, containing 10 mM EDTA as indicated by Brenowitz (1984).

Preparation of Monoclonal Antibodies. (*A*) *Mice and Immunization Procedure.* Balb/cXC57Bl/6 F1 hybrid mice and NZB mice were obtained from the Centre de Sélection et d'Elevage des Animaux de Laboratoires (C.S.E.A.L., CNRS, 45045 Orléans) and were immunized when 3–6 months old. These mice were used instead of the Balb/c mice as donors for immunocompetent cells for fusion because of their higher yield in hybrid cells (G. Motta, unpublished results). Athymic nu/nu mice for ascite production also originated from the C.S.E.A.L.

The antigens used for immunization were purified Aa 2 and Aa 6 subunits. In order to remove traces of contaminating subunits, they were submitted to a preparative cross-line immunoelectrophoresis against an antiserum directed vs. dissociated *A. australis* hemocyanin. At the end of the immunoelectrophoretic migration, the plate was 3 times washed with saline, and then the agarose strip containing the precipitate line corresponding to the subunit was cut out and homogenized in saline. The mice received, with a 10-day interval, two intraperitoneal injections of this homogenate each containing 50–200 μg of antigen. Three days after the second injection the mice were sacrificed, and their spleen cells were used for fusion.

(*B*) *Cell Line and Media.* The myeloma cell line SP2/O/Ag-14 (SP2), a nonsecreting hybridoma derivative originally developed by Shulman et al. (1978), was used throughout all these experiments. The cells were maintained in a complete culture medium called nonselective ERCS (Eagle minimal medium MEMO 111, Eurobio, Paris) reinforced with double amounts of amino acids, vitamins, and glucose and supplemented before use with 2 mM glutamine, 1 mM sodium pyruvate, 10% horse serum (M.A.B.I. Products), and an antibiotic–antimycotic solution. In addition, the ERCS selective medium against SP2 contained 10 μM azaserine and 50 mM hypoxanthine according to Buttin et al. (1978). The sensitivity of SP2 cells to this medium was regularly checked.

(*C*) *Protocol for Fusion, Cloning, and Subcloning.* The fusions between exponentially growing SP2 cells (10 million) and immunized spleen cells (100 million) were carried out according to Gefter et al. (1977) with the following modifications. First, the poly(ethylene glycol) 1000 (Merck 9729) concentration was 50% instead of 30%. Second, after the fusion, 0.1-mL cell fractions approximately containing 100 000 spleen cells were distributed in round-bottomed microtitration plaques, and 0.1 mL of selective medium was added to each fraction. Third, the medium remained unchanged until the clones had grown enough to be tested (10–17 days after the fusion). Then, the medium was progressively replaced by ERCS medium supplemented with hypoxanthine and, 1 week later, by nonselective ERCS medium. Freezing in liquid nitrogen and subcloning of the positive clones by the limiting dilution method were done as soon as possible, to prevent the loss of hybridomas. Successive subclonings of positive subclones were repeated until the hybridoma was stabilized (one to four subclonings). Stable hybridomas were grown into pristane-primed nude or F1 hybrid mice (1 million cells injected intraperitoneally), and the ascitic fluids and sera were collected when ascites had developed.

(*D*) *Screening for Hybridomas.* Two methods were used. In the first method, the proteins present in the culture supernatants were immobilized on a [(Diazobenzyl)oxy]-methyl-(DBM-) activated paper for 2 h at room temperature. The uncovered sites were saturated by immersion of the paper in a 1% (w/v) solution of bovine serum albumin in 1 M glycine for 2 h at 37 °C. Then, the bound material was allowed to react with ^{125}I-labeled hemocyanin subunits for 2–3 h at 4 °C. The paper was then washed overnight in tap water, and the immunocomplexes were detected by autoradiography according to Locker & Motta (1983).

[1] Abbreviations: DBM, [(diazobenzyl)oxy]methyl; EDTA, ethylenediaminetetraacetic acid; ELISA, enzyme-linked immunosorbent assay; EM, electron microscopy; ERCS, Eagle's reinforced complete medium with horse serum; IE, immunoelectrophoresis; mAb, monoclonal antibody; MIEM, molecular immunoelectron microscopy; PAGE, polyacrylamide gel electrophoresis; PBS, phosphate-buffered saline; TLG, thin-layer gel filtration; Tris-HCl, tris(hydroxymethyl)aminomethane hydrochloride.

The second method was a classical ELISA system (monoclonal antibody screening system, New England Nuclear NEI 604) using an alkaline phosphatase conjugated sheep anti-mouse immunoglobulin preparation and immuno-microtitration plates coated with hemocyanin subunits. The experimental conditions were those recommended by the manufacturer.

(*E*) *Determination of the Immunoglobulin Class.* The class of the monoclonal antibodies was determined by Ouchterlony double diffusion in agarose with goat anti-IgM, anti-IgG, anti-IgG_1, anti-IgG_{2A}, and anti-IgG_3 from Nordic Inc.

(*F*) *Titration of Ascitic Fluids.* The titration of the monoclonal antibodies in the ascitic fluid was achieved by the ELISA method described above. Titers are expressed as the reciprocal of the highest dilution of ascitic fluid producing a positive reaction in ELISA.

(*G*) *Preparation of Monoclonal Fab Fragments.* Prior to the preparation of Fab fragments, monoclonal IgG were purified through a gel filtration of the ascitic fluid on Bio-Gel A-1.5m, in a 0.1 M phosphate buffer, pH 6.4. Then, the papainolysis step was conducted according to the method of Porter (1959), and the Fab fragment solution was overnight dialyzed against a 0.05 M Tris-HCl buffer, pH 7.5, containing 0.15 M NaCl. The removal of phosphate ions was found necessary to prevent the precipitation of calcium phosphate during the immunolabeling process.

Immunoelectrophoreses. Crossed immunoelectrophoreses, line immunoelectrophoreses, and crossed-line immunoelectrophoreses were carried out according to the methods of Axelsen et al. (1973). The rabbit antisera directed vs. dissociated hemocyanin or vs. isolated subunits were prepared as previously reported (Lamy et al., 1979b). When an immunoelectrophoresis was the preliminary step of an immunoblotting, the immunoprecipitate was washed for 15 min twice with saline and once with water prior to the first step of the immunoblotting.

Polyacrylamide Gel Electrophoreses. Polyacrylamide gel electrophoreses (PAGE) were carried out in gel slabs containing 7% acrylamide monomer and 0.185% bis(acrylamide). All the other conditions were those recommended by Davis (1964) except that prior to the deposit over the stacking gel the sample was dissolved in the Tris-HCl buffer, pH 6.7, containing 10% glycerol. The sample deposit contained on average 2.5 μg of each subunit (20 μg of dissociated hemocyanin). Subsequent to the electrophoretic migration, proteins were stained with Coomassie G-250, or the gels were used to characterize the antibodies by the blotting procedure.

Detection of Soluble Immunocomplexes by Thin-Layer Gel Filtration. Soluble radiolabeled immunocomplexes were produced by incubating 5 μL of ascitic fluid with 5 μL of ^{125}I-labeled subunit and 15 μL of a 70 g/L bovine serum albumin solution. After a 1-h incubation at 37 °C, the reaction mixture was left overnight at 4 °C; then, the immunocomplexes were separated from IgG and free subunits by thin-layer gel filtration (TLG) on Sephadex G-200 SF in a 0.05 M Tris-HCl buffer, pH 7.5, containing 0.15 M NaCl. Finally, the TLG plate was used in autoradiography with medical X-ray film and α8RA4609 screens from 3M. After a 48-h exposure at −60 °C, the film was developed with reagents recommended by the manufacturer. These conditions were found satisfactory for deposits with radioactivity values as low as 1000 cpm.

Detection of Soluble Immunocomplexes by Immunoblotting. The specificity of the monoclonal antibodies for the various subunits of *A. australis* hemocyanin was determined by modifications of the immunoblotting method of Southern (1975). In a first step, the subunits present in dissociated hemocyanin were separated by PAGE or by immunoelectrophoresis (IE) as described above. In a second step, the polyacrylamide (PAGE) or the agarose (IE) gel slabs were 3 times immersed for 5 min, under slow rotative stirring, in a 10 mM Tris-HCl buffer, pH 7.0, containing 2 mM EDTA and 50 mM NaCl (transfert buffer). Then the free subunits (PAGE) or the precipitated subunits (IE) were transferred to a nitrocellulose membrane (Schleicher & Schüll, BA85 ref 401180) according to the method of Perferoen et al. (1982). After the transfer, in order to saturate the remaining binding sites, the nitrocellulose membrane was surcoated with 3% calf skin gelatin (Sigma ref G-0510) in PBS buffer, pH 7.6, for 1 h at 40 °C (Midgley et al., 1980). Subsequently, the membrane was washed 3 times with PBS buffer containing 0.25% gelatin and 0.2% Tween 20 (washing buffer).

In the third step, the anti-hemocyanin monoclonal antibodies (ascitic fluid 1/250 diluted), called the primary antibody, were bound to the immobilized subunits through a 1-h incubation at 37 °C. Then, the membrane was washed 3 times with the washing buffer to remove the unbound antibodies.

The last step was a detection of the primary antibodies bound to the subunits. For this purpose, a peroxidase-conjugated rabbit immunoglobulin preparation specific for mouse immunoglobulin (Dako ref P161), called secondary antibody, was 1/100 diluted in the washing buffer and incubated for 1 h at 37 °C with the membrane. After thrice washing for 10 min with the washing buffer, the presence of the peroxidase was detected by staining the membrane with a peroxidase reagent (0.05 M Tris-HCl buffer, pH 7.5, containing 50 mg % 3,3′-diaminobenzidine and 0.01% of hydrogen peroxide).

Electron Microscopy. Specimens for electron microscopy and immunoelectron microscopy were prepared by negative staining with 2% uranyl acetate. The specimens were observed in a Jeol 1200 Ex electron microscope at an accelerating voltage of 80 kV. In the microscope, the grid was oriented upside down with the carbon film facing the electron beam and the molecules facing the emulsion side of the photographic film. This procedure restores the correct orientation of the molecule on the print.

Image Processing. The electron microscopic views of the quarters of molecules of *L. polyphemus* hemocyanin were quantitatively analyzed by image processing. The micrographs were scanned with a Perkin-Elmer flat-bed microdensitometer at 50 μm, corresponding to a sampling resolution of 0.1 nm on the object scale. One hundred four images were selected and subjected to computer alignment (Frank et al., 1978). Correspondence analysis (Van Heel & Frank, 1981; Frank et al., 1982; Frank & Van Heel, 1982) was used to determine the presence of systematic trends in the interimage variation. Subsets of molecule images selected by this procedure were averaged and displayed with a limiting resolution of 1.7 nm.

Immunoelectron Microscopy. Immunolabeling was carried out according to a previously published method (Lamy et al., 1981) with the following modifications. For the labeling of whole hemocyanin by monoclonal antibodies (IgG or IgM), 130 μg of whole hemocyanin in a 0.05 M Tris-HCl buffer, pH 7.5, containing 10 mM calcium chloride, was incubated for 1 h at 37 °C with 10 μL of ascitic fluid. Then, the incubation mixture was left overnight at 4 °C. The immunolabeling by monoclonal Fab fragments occurred under the same conditions except that the ascitic fluid was substituted with the Fab fragments preparation. In order to prevent a reassembly of oligomers during the labeling of free subunits, the buffer did not contain calcium ions. Whatever their origin, the immu-

nocomplexes were purified by gel filtration on a Bio-Gel A-1.5 m microcolumn (30 cm in height and 5 mm in diameter) in the incubation buffer. The elution pattern was recorded at 280 nm, and 0.5-mL fractions were negatively stained and examined in the electron microscope.

Results

Architecture of the (4 × 6)-mers. The immunomicroscopic observation of an antibody molecule or of a fragment of antibody molecule bound to a small area of the external surface of an antigen is now perfectly operational and has been applied to a variety of molecules. However, the precision of the immunomicroscopic localization mainly depends on the correctness of the molecular architecture. For the highly complex hemocyanin [(4 × 6)-mers and (8 × 6)-mers], for which the three-dimensional structure has not yet been solved by X-ray crystallography, the models of architecture used to interpret the immunolabeling experiments were mainly deduced from electron microscopy. Such models must be periodically reexamined to take into account the most recent observations. This procedure is especially important in this study because of the high resolution of the labeling with monoclonal antibodies.

Since the publication of our last model of architecture (Lamy et al., 1982), two important new pieces of information have come out. The first one is the discovery by Van Heel et al. (1983) of the 45° view of the (4 × 6)-mer; the second one is the X-ray crystallographic structure of the hexameric hemocyanin of the spiny lobster *P. interruptus* by Gaykema et al. (1984). These data lead to one change and two refinements in the previously published models of (4 × 6)-mer and (8 × 6)-mer architectures.

The change is the substitution of the dodecameric building block of the left enantiomorphic type in the nomenclature of Lamy et al. (1982) with a dodecamer of the right type. The reason for this change is that the stain-exclusion pattern of the 45° view described by Van Heel et al. (1983) is not compatible with the previous model. The impact of the 45° view on the model building will be discussed below.

The refinements are the discrimination between the N- and C-terminal flat faces and the N- and C-terminal domains of the subunits. They were introduced to take into account the results of Gaykema et al. (1984). Actually, these authors have demonstrated that in *P. interruptus* hemocyanin the N- and C-terminal amino acids are located on the two opposing flat faces of the subunits. In addition, the subunits of the upper and lower layers have their C-terminal flat faces in contact, meaning that only their N-terminal and lateral faces are accessible from outside. Furthermore, the subunits are composed of three domains called N terminal, central, and C terminal with respect to their position in the sequence. The fact that the upper trimer is 60° rotated with respect to the lower one results in a superposition of the N-terminal domains in the two trimeric layers. The same superposition pattern is of course observed with the C-terminal domains. The consequence of this configuration is an alternation of superposed N-terminal domains and of superposed C-terminal domains when the molecule is viewed from its 3-fold pseudocrystallographic axis.

This configuration is probably general in arthropod hemocyanins. Indeed, it is also observed in the dodecamers resulting from a limited dissociation of *L. polyphemus* hemocyanin. We analyzed 104 electron microscopic views of the (2 × 6)-mers using correspondence analysis and image averaging (Van Heel & Frank, 1981; Frank & Van Heel, 1982). Our results (Figure 1A,B,D) agree with earlier findings by Van Heel et al. (1983); however, the details relevant to the placement of

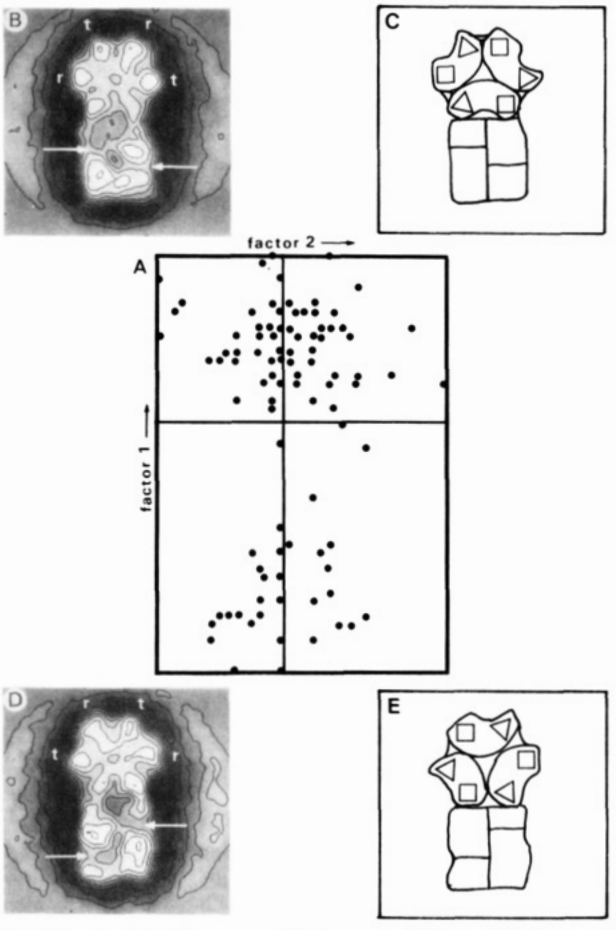

FIGURE 1: Averaged images of the two populations of dodecameric views of *Limulus polyphemus* hemocyanin selected by the correspondence analysis method of Van Heel and Frank. (A) Distribution of the images along the first two factors; (B and D) averaged images of the upper and lower populations of molecules, with positive and negative values along factor 1, respectively. Symbols *r* and *t* refer to the rectangular and triangular shape of the vertices of the upper hexamer. The arrows point to the cleft of minimal stain exclusion in the lower hexamer. (C and E) Schematic patterns of stain exclusion produced by a model of dodecamer of the right enantiomorphic type.

subunits are not discernible in the averaged projections of that study. Two populations of molecules segregate on the map relating to the two main factorial axes. Average images of these populations (Figure 1B,D) clearly correspond to the molecule standing on its opposing faces. Indeed, the salient features of these images are mirror related. In both average images, the upper hexamer, viewed from its 3-fold axis, appears with hexagonal outline while the lower hexamer, viewed from one of its 2-fold axes, appears with rectangular outline. In the hexagon, the vertices labeled *r* and *t* have a rectangular and a triangular boundary, respectively. The pattern must be put side by side with the alternation of the superposed N- and C-terminal domains in *P. interruptus* hemocyanin.

In the rectangular view of the hexamer, two domains of low stain exclusion appear, one on the left and one on the right (arrows), the left domain being always shifted upward or downward with respect to the right one. These domains correspond to the intersubunit clefts of each trimer in contact with the carbon film. In the average image of the upper population of molecules (Figure 1B), the sequence of the vertices of the hexagon can be summarized, from left to right, as *r–t–r–t*, and the left zone of low stain exclusion is shifted upward. In the average image of Figure 1D, the pattern is inverted with a hexagonal sequence of the type *t–r–t–r* and a left cleft shifted downward.

Table I: Origin and Characteristics of Ten Mouse Monoclonal Antibodies Specific for Subunits Aa 2 and Aa 6 of *Androctonus australis*

name[a]	injected antigen	strain of mice immunized	no. of subclonings	titer[b]	class
5701	Aa 6	NZB	2	100000	IgG
5705	Aa 6	NZB	2	10000	IgM
5802	Aa 6	Balb/CXC57B1/6	2	10000	IgM
5804	Aa 6	Balb/CXC57B1/6	2	20000	IgG_1
5808	Aa 6	Balb/CXC57B1/6	2	10000	IgM
6014	Aa 2	NZB	4	100000	IgG_{2A}
6107	Aa 2	Balb/CHC57B1/6	4	10000	IgG_1
6302	Aa 2	Balb/CHC57B1/6	2	1000000	IgG_1
6303	Aa 2	Balb/CHC57B1/6	2	100000	
6304	Aa 2	Balb/CHC57B1/6	2	50000	

[a] The first two characters refer to the fusion number and the last two to the serial number of the hybridoma. [b] Expressed as the reciprocal of the highest dilution giving a positive reaction in ELISA.

In a model of the dodecamer composed of two copies of the right enantiomorphic type (Figure 1C,E), the rectangular boundary of the hexagon vertices corresponds to the superposition of the N-terminal domains. Such a model is in agreement with details of Gaykema's et al. results (1984). Indeed, in the hexamer the N-terminal domain protrudes more outside the triangular envelope of the C-terminal domains than the C-terminal domains do outside the N-terminal domain envelope. Moreover, the size of the N-terminal domain appears larger than the size of the C-terminal domain. This pattern seems in agreement with the conclusion that the N-terminal domain is responsible for a higher stain exclusion, and that it causes a vertex with rectangular boundary to be observed.

Derivation of Anti-Hemocyanin Hybridomas. Seventeen fusions between 17 mice immunized with Aa 2 or Aa 6 and SP2 myeloma cells produced 44 anti-Aa 6 and 40 anti-Aa 2 hybridomas, as evidenced by their reaction in the ELISA and/or DBM screening tests described above. Five stabilized hybridomas of each specificity were selected for this study on the basis of their high antibody titer and rate growth. The origin and the main characteristics of these ten clones are shown in Table I. The titers of the ascitic fluids, expressed as the reciprocal of the highest dilution factor producing a positive reaction, are high for all the clones ranging between 10000 and 1000000. As expected from the short immunization schedule, the antibody classes were IgG or IgM. It should be pointed out that the selection procedure makes it impossible that two different antibody clones arise from the same cell fusion, because a single hybrid was selected from each culture well. However, independently raised clones may recognize, by chance, similar or identical determinants in the same hemocyanin subunit or in structurally related subunits.

Intrasubunit Localization in Native Hemocyanin of an Epitope Present in Subunit Aa 2. Monoclonal antibody 6302 (mAb 6302) was characterized by its ability to bind subunit Aa 2 with high affinity and high specificity. The high affinity of the antibody to antigen binding was demonstrated by thin-layer gel filtration and autoradiography. In a first step, the ascitic fluid was incubated with pure ^{125}I-labeled subunit Aa 2. Then, the radiolabeled immunocomplexes were separated from the free subunits by thin-layer gel filtration on

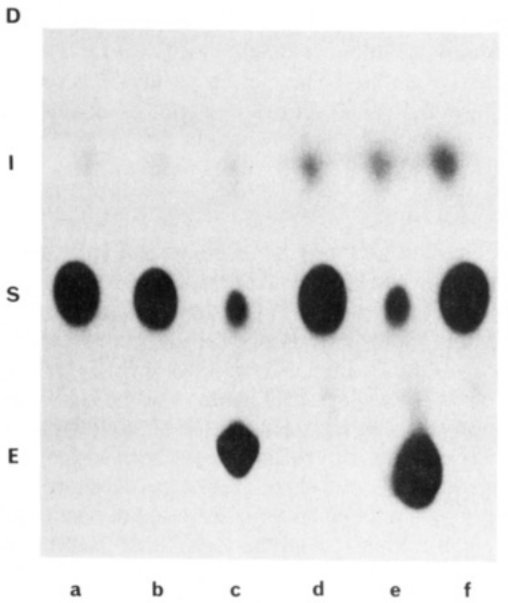

FIGURE 2: Demonstration of the high affinity of 6302 and 5701 monoclonal antibodies for their antigens by thin-layer gel filtration and autoradiography. D, deposit; I, iodine spot; S, free subunit; E, excluded spot (immunocomplex). (a–c) Subunit Aa 2; (d–f) subunit Aa 6; (b and e) mAb 5701; (c and f) mAb 6302.

Sephadex G-200 SF. Finally, the presence of subunit Aa 2 was detected by autoradiography. Figure 2 shows that subunit Aa 2 produces an excluded complex with mAb 6302 while free subunit Aa 2 produces a retarded spot. The presence of an excluded spot qualitatively demonstrates the high strength of the immunocomplex. Indeed, unstable or weakly stable immunocomplexes, such as those produced by mAb 6107 and subunit Aa 2, dissociated during the gel filtration, producing an imprecise trail between the subunit and the material excluded from the gel.

Since strong cross-reactivities and important sequence homologies occur between the various subunits of arthropod hemocyanins, it was important to determine whether or not mAb 6302 was capable of binding to any subunit other than subunit Aa 2. The hypothesis was investigated by the thin-layer gel-filtration method described above. For example, Figure 2 shows that mAb 6302 produces an excluded spot with subunit Aa 2 but not with subunit Aa 6. Conversely, mAb 5701 binds subunit Aa 6 but not subunit Aa 2. None of the six other radiolabeled subunits from *A. australis* hemocyanin produced any excluded immunocomplex with mAb 6302 nor with mAb 5701. The specificity of mAb 6302 was also screened by two modifications of the immunoblotting method of Southern (1975). In the first technique, designated as PAGE immunoblotting, the various free subunits were submitted to PAGE either in a pure form or as dissociated hemocyanin. Subsequently, they were transferred to a nitrocellulose sheet by blotting, and the membrane was allowed to react with the mAb. Finally, the presence of the mAb bound to the subunit was revealed by a peroxidase linked to an anti-mouse IgG preparation. Figure 3 shows the results of this experiment. Tracks 1, 7, and 8 contained dissociated hemocyanin; tracks 2–6 contained equal amounts of pure subunits Aa 6, 5A, 4, 3B, and 2. Clearly, subunits Aa 3B, 4, 5A, and 6 did not produce any coloration with mAb 6302. The same absence of coloration was obtained with subunits Aa 3A and 3C-5B in another experiment. Track 6 shows that subunit Aa 2 produced one major and three minor bands. These four bands all correspond to immunologically and chemically pure subunit Aa 2 as demonstrated by immunoelectrophoresis and

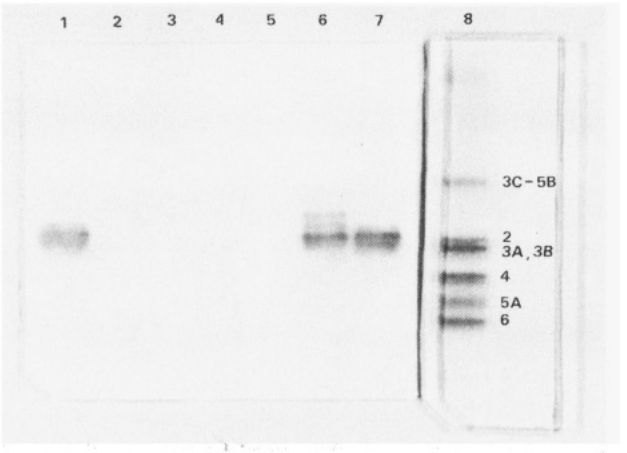

FIGURE 3: Demonstration of high specificity of mAb 6302 for subunit Aa 2 by PAGE immunoblotting: (tracks 1, 7, and 8) 20 μg of dissociated hemocyanin; (tracks 2–6) 2.5 μg of subunits Aa 6, 5A, 4, 3B, and 2; (tracks 1–7) nitrocellulose sheet stained for peroxydase activity; (track 8) part of the polyacrylamide gel slab stained with Coomassie G-250.

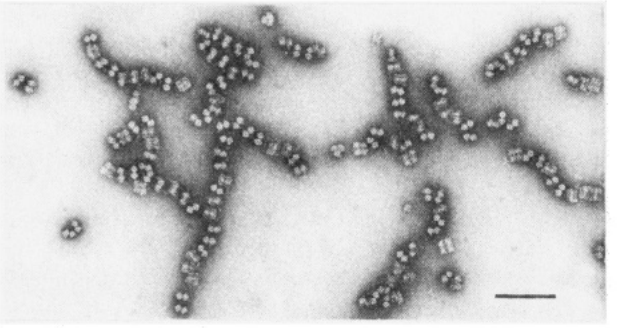

FIGURE 4: Molecular immunoelectron microscopy of whole *Androctonus australis* hemocyanin labeled with mAb 6302. The length of the bar is 100 nm.

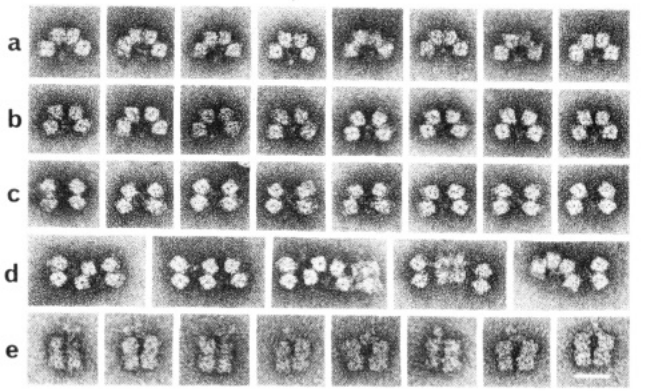

FIGURE 5: Enlargements of characteristic immunocomplexes between *Androctonus australis* hemocyanin and mAb 6302 obtained at a high antigen to antibody ratio. (a–c) Complexes composed to two hemocyanin molecules; (a) parachute; (b) intermediate; (c) butterfly; (d) complexes containing three or four hemocyanin molecules; (e) complexes containing a single hemocyanin molecule. The bar corresponds to 25 nm.

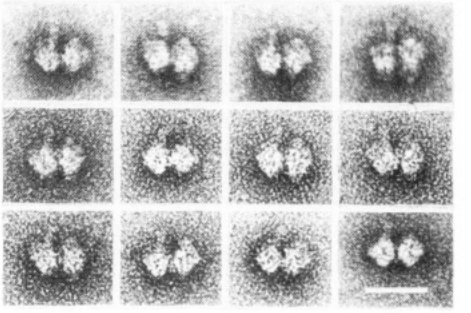

FIGURE 6: Immunolabeling of *Androctonus australis* hemocyanin by monoclonal Fab fragments prepared from mAb 6302. Notice that the Fab fragments are visible on the outline near the top edge of the left dodecamer and the bottom edge of the right dodecamer. The bar is 25 nm.

N-terminal sequence determinations (Lamy et al., 1979a; Jollès et al., 1979). Since dissociated hemocyanin produces a doublet in PAGE, the additional heterogeneity observed with purified subunit Aa 2 was likely caused, during the purification, by minor conformational changes that slightly altered the net charge of the subunit without strongly affecting its immunological properties.

The apparent high specificity of mAb 6302 for subunit Aa 2 was confirmed by a semiquantitative method called dot blotting. In this method, increasing amounts of pure subunits were deposited as small droplets directly on the nitrocellulose membrane producing small antigen dots. Then, the membrane was incubated with the ascitic fluid 1/250 diluted, and the immunocomplexes were stained as above. The results showed that no subunit other than Aa 2 was stained even at concentrations 100 times higher than the optimum Aa 2 concentration. At an antigen concentration 1000 times higher, a faint unspecific coloration appeared with all the subunits. A repetition of this experiment with ascitic fluid dilutions ranging from 1/50 to 1/2500 produced the same results, confirming that the epitope of mAb 6302 is only present in subunit Aa 2.

The localization of the mAb 6302 epitope within native *A. australis* hemocyanin was carried out by MIEM. Two methods producing different types of immunocomplexes were used. In the first method, whole hemocyanin was incubated with the mAb 6302 containing ascitic fluid, and the immunocomplexes were freed from low molecular weight components by gel filtration on Bio-Gel A-1.5m. As shown in Figure 4, the immunocomplexes appear as long strings composed of whole hemocyanin molecules mostly in the side view and in the 45° view. The hemocyanin molecules are not brought into contact, and extra material is clearly seen between them. Immunocomplexes smaller in size obtained at a lower antibody concentration are shown in Figure 5. Many of them were composed of two hemocyanin molecules in their side views sitting side by side (Figure 5a) or parallel (Figure 5c), producing structures denoted as "parachute" and "butterfly", respectively, which clearly are the building blocks of the strings of Figure 4. Figure 5b shows intermediate forms between the parachute and the butterfly forms, suggesting that there is a continuous variation between the two main forms. Much less frequent were forms containing one (or two) hemocyanin molecule(s) in the top view. These forms, shown in Figure 5d,e, were as a rule more or less distorted, suggesting that interactions with the support film induced strong tensions that caused important conformational changes. The appearances of all these immunocomplexes suggest that the mAb 6302 epitope is located near the top/bottom edges of the (4 × 6)-mer. The linearly ordered immunocomplexes of Figure 4 demonstrate that the four copies of the epitope are distributed in the two faces of the molecule, as expected from the intramolecular location of subunit Aa 2. However, the resolution of the method was not good enough to localize the attachment point of the monoclonal antibody.

The binding point of mAb 6302 onto subunit Aa 2 was more precisely determined by substituting monoclonal IgG's with monoclonal Fab fragments. Because of the monovalence of

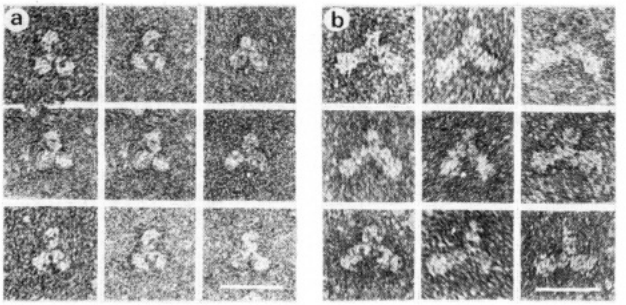

FIGURE 7: Gallery of (a) mAb 6003 and (b) immunocomplexes between mAb 6003 and pure subunit Aa 2. The length of the bar is 25 nm.

Fab fragments, this second method did not produce any more of the stringlike structures but immunocomplexes containing a single hemocyanin molecule. Figure 6 shows that the Fab fragments were located almost exactly on the top edge of the left dodecamer and/or on the bottom edge of the right dodecamer. It is highly relevant to our problem that Fab fragments were seen only on the outline of the side view and that their orientation was roughly perpendicular to the general plane of the molecule. The fact that only two Fab fragments are visible while there are four copies of subunit Aa 2 per (4 × 6)-mer may be explained by partial staining of the molecule, contrasting the side facing the carbon grid preferentially and producing complete stain exclusion only for Fab fragments in close contact with the grid. The position of the fragments on the top of the structure, where subunit Aa 2 is known to be located, is least favorable for their visualization in our single-layer preparation. Indeed, it is well-known that when an object lying on a carbon film is negatively stained, the bottom side and the top side of the object may be differently stained. The bottom side in contact with the film produces a strong stain exclusion giving a sharp contour line. Conversely, the top side may be outside of the stain layer and therefore not visible. This loss of information due to partial staining effect is especially important with objects of which the height is large compared to the thickness of the stain layer (Frank et al., 1982; Moody, 1967).

The location of the Fab fragments on the top and bottom edges of the left and right dodecamers will be discussed below. However, it can be noticed here that the agreement between the MIEM views and the model is fairly good (see Figure 12).

Case of an Epitope Present in Subunit Aa 2 but Masked or Absent in Native Hemocyanin. mAb 6003 was characterized by PAGE immunoblotting and by TLG followed by autoradiography. Both methods led to the conclusion that this clone has a high specificity and a high affinity for subunit Aa 2. However, no immunocomplexes could be observed after immunolabeling native hemocyanin with monoclonal IgG's nor with monoclonal Fab fragments. The fact that mAb 6003 was capable of producing soluble immunocomplexes with subunit Aa 2 was confirmed as follows by MIEM. Pure free subunit Aa 2 was incubated with the ascitic fluid; then, the immunocomplexes were purified by gel filtration and examined in the electron microscope. Figure 7 shows selected views of monoclonal IgG's and of immunocomplexes clearly composed of one IgG molecule binding two copies of subunit Aa 2. Therefore, it can be concluded that in native hemocyanin either the epitope is not accessible to the antibody or that it has been destroyed upon subunit aggregation.

Case of Monoclonal IgM's and Low-Affinity IgG's. The various fusions produced many monoclonal IgM's. However, most of them were not useful or of little interest for three reasons. First, the immunocomplexes were very difficult to separate from unbound IgM's. Therefore, it was impossible to rule out that the few putative immunocomplexes observed were artifacts. Figure 8 shows such possible immunocomplexes obtained with mAb 6301, an antibody directed vs. subunit Aa 2. The contact point between the IgM molecule and the hemocyanin molecule(s) is in good agreement with the location of subunit Aa 2. However, due to the polymorphism of the IgM molecules, the binding point was too imprecise to allow a localization of the epitope within the subunit. The second reason why monoclonal IgM's were not useful was the difficulty of splitting them into fuctional Fab fragments [see Goding (1983) for more details]. The last reason was that monoclonal IgM often produced weak immunocomplexes that dissociated during the purification. These reasons made us discontinue use of monoclonal IgM for labeling hemocyanin in our laboratory.

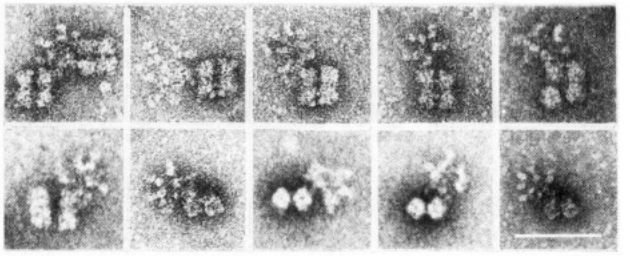

FIGURE 8: Gallery of possible immunocomplexes between *Androctonus australis* hemocyanin and monoclonal IgMs (mAb 6301). The length of the bar is 50 nm.

Low-affinity IgG, such as mAb 6107 or 6304, could not be used in MIEM. Actually, though their binding to hemocyanin subunits was clearly demonstrated by immunoblotting, the immunocomplexes continuously dissociated during the gel filtration. As described above, the dissociation produced a trail in thin-layer filtration between the material excluded from the gel and the free subunits. The same phenomenon probably occurred during the gel filtration of mAb incubated with the whole hemocyanin. However, when observed in the electron microscope, the fractions corresponding to the excluded material and to the trail never showed characteristic definite immunocomplexes. Therefore, the low-affinity monoclonal IgG's are no longer used for MIEM in our laboratory.

Immunolabeling in Native Hemocyanin of an Epitope of Subunit Aa 6: A Demonstration of the High Rotational Flexibility of Monoclonal IgG's. As described above, mAb 5701 was characterized by TLG and autoradiography. Figure 2 shows that the immunocomplexes excluded from the gel were as stable as those formed between mAb 6302 and subunit Aa 2. Their specificity for subunit Aa 6, determined by PAGE immunoblotting and by TLG plus autoradiography was perfect.

MIEM of native hemocyanin by mAb 5701 was carried out as described above. Figure 9 shows a micrograph of the fraction excluded from Bio-Gel A-1.5m. This fraction contained soluble immunocomplexes and unlabeled hemocyanin molecules. The background was very clean and completely free of residual IgG molecules. Only some α_2-macroglobulin molecules can be sporadically seen. Though the size of the immunocomplexes was much smaller than those with mAb 6302, their frequency compared to the residual molecules was not negligible. At the high magnification of Figure 10, the binding point of the IgG molecule is obviously in the corners of the hemocyanin (4 × 6)-mer, exactly in the area where subunit Aa 6 is known to be located (Lamy et al., 1981). The soluble immunocomplexes can be classified into two different types differing by the angle between the two Fab arms in the

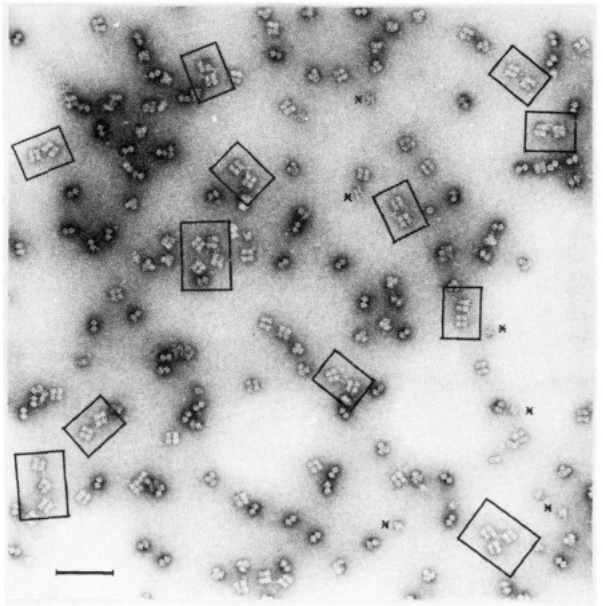

FIGURE 9: Micrograph of the soluble immunocomplexes between mAb 5701 and (4 × 6)-meric hemocyanin from *Androctonus australis*. The stars show α_2-macroglobulin molecues from the ascitic fluid excluded from the gel during the gel filtration. The length of the bar is 100 nm.

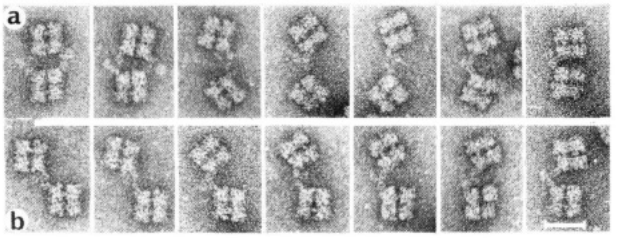

FIGURE 10: Selected views of the soluble immunocomplexes produced by mAb 5701 with *Androctonus australis* hemocyanin: (a) first type; (b) second type. The length of the bar is 25 nm.

IgG molecule and by the rotation angle around the long axis of the Fab fragment. If the contact between the antibody site of the Fab and the antigen is supposed to be tight (high affinity), the values of the angle between the two Fab arms can be approximately deduced from the orientation of the longitudinal clefts of the two hemocyanin molecules and from the contact point between the Fabs and the hemocyanin molecules. The first type of immunocomplexes corresponds to views shown in row a in Figure 10. For example, the two complexes on the left of Figure 10a are clearly composed of two hemocyanin molecules and two monoclonal IgG molecules. The longitudinal clefts of the hemocyanin molecules are almost perfectly aligned. Conversely, in the last view on the right, the clefts are almost parallel. Other views of row a show a continuous transition between these two extreme views. The existence of all these complexes can be explained by the segmental flexibility of the IgG in the hinge area and by a low degree of rotational flexibility of the Fab arm. This is illustrated by the model of Figure 12, which shows that the N-terminal flat faces of the four copies of subunit Aa 6, have different orientations with respect to the carbon film. The N-terminal faces of the subunits oriented toward the carbon film define the direction of the rocking axis (Van Heel & Frank, 1981). Conversely, the N-terminal faces of the other two subunits are facing away from the carbon film. In complexes of the first type (Figure 10, row a), the two Fab arms of the mAb are bound to epitopes with different orientations.

In the second type of complexes (Figure 10, row b), the transition between the various views is also easily explained by the assumption of segmental flexibility at the hinge. However to pass from immunocomplexes of the first to the second type, it is necessary to postulate a high degree of rotational flexibility (twisting) around the Fab axis either between the variable and constant domains or in the hinge area. This rotation is also demonstrated by the orientation of the subunit's flat faces linked by the two Fab arms of the mAb, as both copies of subunit Aa 6 have the same orientation with respect to the carbon film. The complexes of Figure 10 also show that the binding point of the antibody to the hemocyanin molecule is located exactly in the corner of the hemocyanin molecule, an area that approximately corresponds to the C-terminal domain in the model of Figure 12.

Discussion

Architecture of the (4 × 6)-meric Hemocyanins. All the previously published models of (4 × 6)-meric hemocyanin were composed of hexamers similar to *P. interruptus* hemocyanin (Lamy et al., 1981b, 1982; Sizaret et al., 1982). The model of the basic hexamer made up of six kidney-shaped subunits assembled in a trigonal antiprism possessed a 3-fold axis of symmetry, but no distinction was made between the flat faces. The recent results of Gaykema et al. (1984) allow this model to be refined, by distinguishing N- and C-terminal faces and N- and C-terminal domains in the subunit. The fact that the C-terminal faces of the two trimeric layers of subunits come into contact in *P. interruptus* explains the alternation of triangular and rectangular boundaries in the outline of the dodecamers of *L. polyphemus* hemocyanin. Moreover, the strong preservation of the amino acid sequence in crustacea and chelicerate hemocyanin subunits (Moore & Riggs, 1983; Nemoto & Takagi, 1983; Schartau et al., 1983; Schneider et al., 1983; Gaykema et al., 1984; Yokota & Riggs, 1984) strongly suggests that the hemocyanin folding first described in *P. interruptus* is general in arthropodan hemocyanin with only minor differences.

The main unresolved problem was to determine the correspondence between the rectangular or triangular boundary visible in the dodecamers of *L. polyphemus* hemocyanin and the N- (or C-) terminal domain. Another approach to the determination of this correspondence would be to establish whether the hexamer association produces dodecamers of the right or left enantiomorphic type in the nomenclature of Lamy et al. (1982). This complex question led to a controversy between M. Van Heel and J. Lamy. Initially, Lamy et al. demonstrated in the (4 × 6)-meric hemocyanin of the scorpion *A. australis* that the interdodecamer bridges link the dimeric subunits (Aa 3C-5B) of both dodecamers (Lamy et al., 1981). At the EMBO Meeting of Leeds (1982),[2] J. Lamy suggested that the contacts should occur between the flat faces of subunits Aa 3C and Aa 5B and that the rocking direction (lower right–upper left) allow determination of the enantiomorphic forms of the dodecamer. He rejected the right enantiomorph because he thought that the rotation of the dodecamer, labeled 1–2 in Figure 13, around the 2-fold axis of the dodecamers should bring into contact the flat faces of the subunits involved in the bridges. However, at the same EMBO Meeting, Van Heel described a new EM view of the (4 × 6)-mer that he called "45° view" (Van Heel et al., 1983). The pattern of stain exclusion of this view was incompatible with the model of Lamy et al. (1982). Indeed, while in the model of Lamy et

[2] EMBO workshop "Structure and Function of Invertebrate Respiratory Proteins", organized by E. J. Wood, Leeds, UK., July 19–22, 1982.

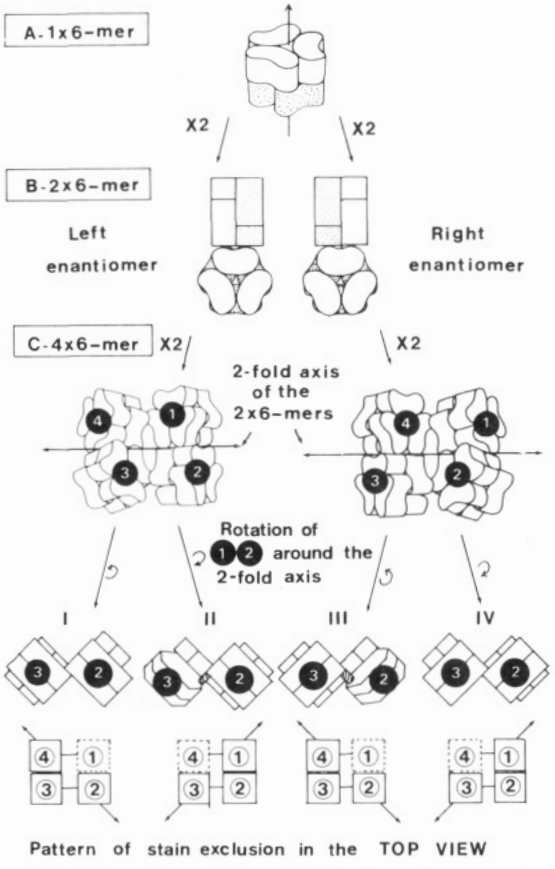

FIGURE 11: Schematic modeling of (4 × 6)-mer hemocyanin from right and left dodecameric enantiomorphs. The numbers 1–4 are used to label the four hexamers only for clarity of the demonstration. Indeed, as long as the shift between the dodecamers has not been introduced, hexamers 1 and 2 are indistinguishable from hexamers 3 and 4, respectively. In the pattern of stain exclusion, the dotted lines and the full lines correspond to a low and a high stain exclusion, respectively.

al. the molecule was standing on its right dodecamer when the longitudinal cleft ws oriented from top to bottom and when the hexamer with a hexagonal contour was oriented to the top of the figure, the pattern of stain exclusion of the molecule was the opposite (greater stain exclusion for the dodecamer on the left).

To take into account this observation and several other minor arguments, the building of the (4 × 6)-mer is completely reexamined in this paper. Specifically, no assumption is made on the rotation direction of the dodecamer composed of hexamers labeled 1 and 2 in Figure 11. The results of this reexamination are depicted in Figure 11. Both dodecameric enantiomorphs can produce (4 × 6)-mers with a rocking axis oriented to the upper left and to the upper right, depending on whether the rotation of the 1–2 dodecamer is clockwise or anticlockwise. The four resulting models are denoted as I–IV in Figure 11. Models II and IV can be rejected because their rocking axis has the wrong direction (to the upper right). Model I can be rejected because it leads to the wrong pattern of stain exclusion in the 45° view. Model III exhibits a rocking axis correctly oriented and correct pattern of stain exclusion. It is composed of two copies of the right enantiomorphic types, the 1–2 dodecamer being rotated anticlockwise around the two-fold axis.

However, some unresolved questions remain. Four example, the nature of the material filling the gap between the dodecamers is not yet clear. It seems unlikely that this could be a low molecular weight subunit. An expansion of the C-terminal domain of the subunit involved in the interdodecamer bridges would be more probable. One or two components of the dimeric subunits Aa 3C–5B of *A. australis*, Ec b–c of *E. californicum*, or Lp V–VI of *L. polyphemus* hemocyanin would be good candidates for having an additional domain or polypeptide loop. Unfortunately, since the dimeric subunits are present in low amount (one copy per dodecamer) and since they are usually difficult to isolate, no sequence data have yet been published.

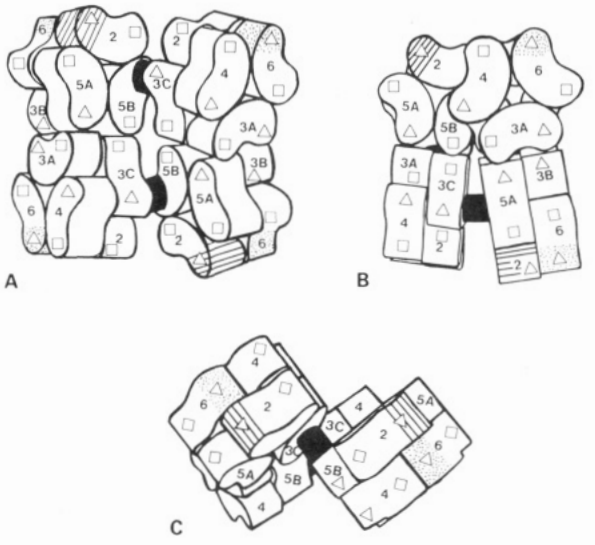

FIGURE 12: Refined model of quaternary structure of *Androctonus australis* hemocyanin showing the proposed location of mAb 6302 and 5701 epitopes: (A) top view; (B) 45° view; (C) side view. The model is built from two copies of the right enantiomorph of the dodecamer. Squares and triangles are used to mark the N-terminal and the C-terminal domains. The dotted area corresponds to the epitope area of mAb 5701 on subunit Aa 6 and the hatched zone of subunit Aa 2 to mAb 6302 epitope.

Another problem is posed by the observation that the 45° view of our model is not in perfect agreement with the corresponding EM views. Indeed, the long axes of the dodecamers are slightly divergent in the model (Figure 12). In contrast, correspondence analysis of a representative population of 45° views shows that only a fraction exhibits the same feature, the other being composed of allmost perfectly parallel dodecamers (Van Heel et al., 1983). The origin of this difference is still unclear.

Consequences of the Reexamination of Hemocyanin Architecture on the Quaternary Structure. The refinements and the change introduced in the dodecamer model to take into account the more recent data lead to some adjustments in the model of the quaternary structure shown in Figure 12. As the model of quaternary structure is used to interpret the MIEM images presented above, these adjustments must be carefully discussed.

In the top view (Figure 12A), the model is standing on its FLOP face and the FLIP (terminology of Sizaret et al., 1982) face is oriented toward the reader. The rocking axis passes from the lower right to the upper left hexamer. Subunits Aa 3B and Aa 5B are located in the long diagonally opposed hexamers and subunits Aa 3A and 3C are in the short diagonally opposed hexamers. In addition, the N- and C-terminal domains of each subunit have been tagged with small squares and triangles, which are meant to symbolize the shapes of their projections in the dodecamer Parts B and C of Figure 12 show the 45° view and the side view of the same model, respectively. The hatched and dotted areas of Figure 12 indicate the tentative intrasubunit location of the epitopes corresponding to

mAb 6302 and mAB 5701, deduced from MIEM. To compare the proposed locations of these epitopes in the model with those in the micrographs of Figures 4–6, 8, 9, and 10, it must be kept in mind that the immunocomplexes shown in the micrographs are imprints of the three-dimensional structure of the model in the stain layer. For example, the hatched area corresponding to the C-terminal domain of subunit Aa 2 in Figure 12C appears near the bottom edge of the left dodecamer and near the top edge of the right dodecamer. Conversely, the corresponding Fab fragments are bound to the top edge of the left dodecamer and to the bottom edge of the right dodecamer in the micrographs of Figure 6.

Is the Rotational Flexibility of the Fab Arm More Important Than Previously Expected? The results described in Figure 10 demonstrate that an important rotation occurs around the long axis of the Fab arm. The phenomenon is in excellent agreement with two similar previously reported observations. Wrigley et al. (1983) purified soluble immunocomplexes composed of monoclonal IgG's and influenza virus hemagglutinin. The electron micrographs of these complexes demonstrate that in addition to the segmental flexibility at the hinge the monoclonal IgG has two other types of flexibility. The first one occurs at the elbow between the variable and constant region of the Fab arm. The second observation is a rotational flexibility that can reach 180° around the long axis of the Fab arm. More recently, Roux (1984) has reported a similar observation on an immunocomplex composed of monoclonal antiallotype Fab fragments and rabbit IgG's. However, the reports of Wrigley, Roux, and this paper employed essentially the same method of MIEM using negative staining of the immunocomplexes. Therefore, one can wonder to what extent the rotation may have been forced by interactions between the protein material and the support film. One way of solving the problem would probably be to observe directly the immunocomplex in suspension in vitreous water (Dubochet et al., 1982).

Future Developments of the MIEM Approach of the Antigenic Determinant Location. The results presented in this paper indicate that an epitope can be localized in one domain of a single hemocyanin subunit. The sizes of the presently known hemocyanin domains vary between 177 and 262 residues (Gaykema et al., 1984). However, not all of these residues are accessible to the antibody because of the globular character of the domain or because of steric hindrance with other subunits in the oligomer. In the specific case of the epitope of mAb 6302, a detailed examination of the model of the C-terminal domain (of *P. interruptus* hemocyanin) shows that less than half of the β-barrel is accessible to antibody and that the two lateral loops located in the concave face are incompatible both with the orientation of the Fab fragments and with the structure of the strings of immunocomplexes of Figure 4. With these restrictions, the number of accesible residues compatible with MIEM views of Figures 4 and 5 is at most of 80. With antigens more asymmetric than hemocyanin subunits, MIEM allows one to directly circumscribe the epitope to a still smaller number of residues (Fab fragments, influenza hemagglutinin).

The orientation of the Fab fragment on the antigen surface should also help to reduce the number of residues possibly involved in the epitope, provided that the extent of the deformation caused by the stain or by interaction with the support is fully understood. Here again, an electron microscopic observation of the complex in vitreous water should strongly improve the results. Actually, in contrast to the negative stain technique, the molecules in suspension in vitreous water are randomly oriented so that there is always a favorable view for the observation of the label.

The results can also be improved by image processing. For example, preliminary experiments of immunolabeling of subunit Lp II by polyclonal Fab fragments show that the attachment point of the label to the hemocyanin molecule can be very accurately determined. Indeed, because of the movement of the Fab fragment around its point of attachment, the averaging produces only a small invariable region. The diameter of this invariable region is much smaller (1 nm) than that of the Fab fragment itself (Frank et al., 1983). Therefore, one can predict that the image processing of the immunocomplexes by the correspondence analysis method should in the near future circumscribe an epitope in an area of the same order of size as the epitope itself. Of course, classical methods will be required to finally localize the determinant, such as comparison of amino acid sequence of structurally related subunits with the mAb affinity, the binding of mAb to synthetic peptides, the destruction of the epitope by iodination, etc. However, the fact that immunolabeling circumscribes the determinant in a small three-dimensional area should considerably simplify this last step. Moreover, the MIEM method is as powerful with conformational (continuous) epitopes as with sequential (discontinuous) epitopes and has no other limitation than the resolution of electron microscopy. This means that improvements in the practical resolution of electron microscopy due to improvements of specimen preparation and contrasting methods will automatically be followed by improvements in the resolution of MIEM.

ACKNOWLEDGMENTS

We are pleased to thank Professor J. C. Besnard (University of Tours) and Dr. D. Guilloteau for teaching radioimmunolabeling of antigens, Professor P. Rouleau (University of Tours) for stimulating discussion about medical X-ray films, and Professor Buttin (Institut Pasteur, Paris) for giving the SP2 myeloma line. We are also grateful to S. Compin and M. Leclerc for their skillful technical assistance.

REFERENCES

Alliel, P. M., Dautigny, A., Lamy, J., Lamy, J. N., & Jollès, P. (1983) *Eur. J. Biochem. 134*, 407–414.

Avissar, I., Daniel, V., & Daniel, E. (1983) *Comp. Biochem. Physiol., B: Comp. Biochem. 75B*, 327–330.

Axelsen, N. H., Kroll, J., & Weeke, B. (1973) *Scand. J. Immunol. 2* (Suppl. 1).

Brenowitz, M., Bonaventura, C., & Bonaventura, J. (1984) *Biochemistry 23*, 879–888.

Buttin, G., Le Guern, G., Phalente, L., Lin, E. C. C., Medrano, L., & Cazenave, P. A. (1978) *Curr. Top. Microbiol. Immunol. 81*, 27–36.

Davis, B. (1964) *Ann. N.Y. Acad. Sci. 121*, 404–427.

Dubochet, J., Lepault, J., Freeman, R., Berriman, J. A., & Homo, J. C. (1982) *J. Microsc. (Oxford) 128*, 219–237.

Ellerton, N. F., Ellerton, H. D., & Robinson, H. A. (1983) *Prog. Biophys. Mol. Biol. 41*, 143–248.

Folkerts, A., & Van Eerd, J. P. (1981) in *Inwertebrate Oxygen Binding Proteins, Structure, Active Site, and Function* (Lamy, J., & Lamy, J., Eds.) pp 215–221, Marcel Dekker, New York.

Frank, J., & Van Heel, M. (1982) *J. Mol. Biol. 161*, 134–137.

Frank, J., Goldfarb, W., Eisenberg, D., & Baker, T. S. (1978) *Ultramicroscopy 3*, 283–290.

Frank, J., Verschoor, A., & Boulbik, M. (1982) *J. Mol. Biol. 161*, 107–133.

Gaykema, W. P. J., Hol, J. M., Vereijken, J. M., Soeter, N. M., Bak, H. J., & Bientema, J. J. (1984) *Nature (London) 309*, 23–29.

Gefter, M. D., Margulies, M., & Scharff, M. D. (1977) *Somatic Cell Genet. 3*, 231–236.

Goding, J. W. (1983) *Monoclonal Antibodies: Principles and Practice*, Academic Press, London.

Greenwood, F. C., Hunter, W. M., & Glover, J. S. (1963) *Biochem. J. 89*, 114–123.

Jeffrey, P., Lamy, J., Lamy, J., Leclerc, M., & Malborough, D. (1981) in *Invertebrate Oxygen Binding Proteins, Structure, Active Site, and Function* (Lamy, J., & Lamy, J., Eds.) pp 227–233, Marcel Dekker, New York.

Jollès, J., Jollès, P., Lamy, J., & Lamy, J. (1979) *FEBS Lett. 106*, 289–291.

Lamy, J., Lamy, J., & Weill, J. (1979a) *Arch. Biochem. Biophys. 193*, 140–149.

Lamy, J., Lamy, J., Weill, J., Bonaventura, J., Bonaventura, C., & Brenowitz, M. (1979b) *Arch. Biochem. Biophys. 196*, 324–339.

Lamy, J., Lamy, J., Weill, J., Markl, J., Schneider, H. J., & Linzen, B. (1979c) *Hoppe Seyler's Z. Physiol. Chem. 360*, 889–895.

Lamy, J., Bijlholt, M. M. C., Sizaret, P.-Y., Lamy, J. N., & van Bruggen, E. F. J. (1981) *Biochemistry 20*, 1849–1856.

Lamy, J., Sizaret, P.-Y., Frank, J., Verschoor, A., Feldmann, R., & Bonaventura, J. (1982) *Biochemistry 21*, 6825–6833.

Lamy, J., Lamy, J., Sizaret, P.-Y., Billiald, P., Jollès, P., Jollès, J., Feldmann, R. J., & Bonaventura, J. (1983) *Biochemistry 22*, 5573–5583.

Locker, D., & Motta, G. (1983) *J. Immunol. Methods 59*, 269–275.

Mangum, C. P., Scott, J. L., Black, R. E. L., Miller, K. I., & Van Holde, K. E. (1984) *Proceedings of the Congress of Comparative Physiology and Biochemistry Section of IUBS, 1st*, ESPCB, Liege, Belgium.

Markl, J., Kempter, B., Linzen, B., Bijlholt, M. M. C., & van Bruggen, E. F. J. (1981) *Hoppe Seyler's Z. Physiol. Chem. 362*, 1631–1641.

Markl, J., Gebauer, W., Runzler, R., & Avissar, I. (1984) *Hoppe Seyler's Z. Physiol. Chem. 365*, 619–631.

Midgley, A. R., Jr., & Hepburn, M. R. (1980) *Methods Enzymol. 70A*, 266–274.

Moody, M. F. (1967) *J. Mol. Biol. 25*, 167–200.

Moore, M. D., & Riggs, A. F. (1983) *Life Chem. Rep., Suppl. Ser. 1*, 93–97.

Nemoto, T., & Takagi, T. (1983) *Life Chem. Rep., Suppl. Ser. 1*, 89–92.

Perferoen, M., Huybrechts, R., & De Loof, A. (1982) *FEBS Lett. 145*, 369–372.

Porter, R. R. (1959) *Biochem. J. 73*, 119–126.

Roux, K. H. (1984) *Eur. J. Immunol. 14*, 459–464.

Schartau, W., Eyerle, F., Reisinger, P., Geisert, H., Storz, H., & Linzen, B. (1983) *Hoppe Seyler's Z. Physiol. Chem. 364*, 1383–1409.

Schneider, H. J., Drexel, R., Feldmaier, G., & Linzen, B. (1983) *Hoppe Seyler's Z. Physiol. Chem. 364*, 1357–1381.

Shulman, M., Wilde, D. C., & Köhler, G. (1978) *Nature (London) 276*, 299–301.

Siggens, K. W., & Wood, E. J. (1982) *Eur. J. Biochem. 131*, 353–358.

Sizaret, P. Y., Frank, J., Lamy, J., Weill, J., & Lamy, J. N. (1982) *Eur. J. Biochem. 127*, 501–506.

Southern, E. M. (1975) *J. Mol. Biol. 98*, 503–517.

Vanderbeke, E., Cleuter, Y., Marbaix, G., Prêaux, G., & Lontie, R. (1982) *Biochem. Int. 5*, 23–29.

Vanderbeke, E., Marbaix, G., Prêaux, G., & Lontie, E. (1983) *Life Chem. Rep., Suppl. Ser. 1*, 385–386.

Van Heel, M., & Frank, J. (1981) *Ultramicroscopy 6*, 187–194.

Van Heel, M., Keegstra, W., Schutter, W., & van Bruggen, E. F. J. (1983) *Life Chem. Rep., Suppl. Ser. 1*, 69–73.

Van Holde, K. E., & Miller, K. I. (1982) *Q. Rev. Biophys. 15*, 1–129.

Wood, E. J. (1983) *Life Chem. Rep., Suppl. Ser. 1*, 365–375.

Wrigley, N. G., Brown, E. B., & Skehel, J. J. (1983a) *J. Mol. Biol. 169*, 771–774.

Wrigley, N. G., Brown, E. B., Daniels, R. S., Douglas, A. R., Skehel, J. J., & Wiley, D. C. (1983b) *Virology 131*, 308–314.

Yokota, E., & Riggs, A. (1984) *J. Biol. Chem. 259*, 4739–4743.